Molecular Crystals and Liquid Crystals
Publication details, including instructions for authors and subscription information:
http://www.tandfonline.com/loi/gmcl16

Optical Properties of Cholesteric Liquid Crystals at Oblique Incidence

E. Miraldi [a] , C. Oldano [a] , P. I. Taverna [a] & L. Trossi [a]
[a] Dipartimento di Fisica, Politecnico di Torino, Italy
Version of record first published: 13 Dec 2006.

To cite this article: E. Miraldi , C. Oldano , P. I. Taverna & L. Trossi (1983): Optical Properties of Cholesteric Liquid Crystals at Oblique Incidence, Molecular Crystals and Liquid Crystals, 103:1-4, 155-176

To link to this article: http://dx.doi.org/10.1080/00268948308071047

Mol. Cryst. Liq. Cryst., 1983, Vol. 103, pp. 155–176
0026-8941/83/1034–0155/$18.50/0

Printed in the United States of America

Optical Properties of Cholesteric Liquid Crystals at Oblique Incidence

E. MIRALDI, C. OLDANO,† P. I. TAVERNA and L. TROSSI

Dipartimento di Fisica, Politecnico di Torino, Italy

(*Received January 31, 1983; in final form March 24, 1983*)

The optical properties of a periodic structure characterized by a uniform rotation of the dielectric tensor about a given axis are theoretically analyzed. The electromagnetic wave is described as a superposition of elementary modes having the form of Bloch waves. Each elementary mode is represented by a sum of plane waves elliptically polarized, whose wavevectors are the solutions of a characteristic equation. This equation, presented in a preceding paper, is furtherly analyzed, in order to obtain the wave vectors in terms of a power series of a small parameter δ, representing the anisotropy of the dielectric tensor. The coefficients of the series up to terms containing δ^6 are explicitly given, and the corresponding truncation errors computed. The spectral composition and the polarization states of the Bloch waves are also analyzed and discussed for different values of the incidence angle in the frequency range containing the lower reflection bands. In particular it is shown that in the regions between the reflection bands both the wave functions and the wavevectors can be evaluated with very good approximation by simple analytic expressions, while for an accurate evaluation of the reflection properties of the structure more involved expressions are needed.

1. INTRODUCTION

The equations for the propagation of light in a perfect cholesteric liquid crystal have simple analytical solutions only when the light is propagating along the helix axis. For the case of oblique incidence the quantities of physical interest are generally evaluated by numerical methods, among which the most used is the 4×4 matrix method.[1]

A different technique for computing some of the optical properties has been used by Taupin,[2] Dreher and coworkers[3] and by Belyankov and Dmitrienko.[4] It consists in finding Bloch waves solutions for the Maxwell equations.

†Gruppo Nazionale Struttura della Materia del C.N.R., U.R.24

In a recent paper[5] the authors used this method to obtain a general equation which gives the wavevectors of the Bloch waves as a function of the frequency and of the incidence angle. The coefficients of this equation depend on a determinant having infinite elements, which has been computed by numerical techniques.

In the present paper it is shown that such a determinant can be expanded in a power series of a small parameter δ, which represents the anisotropy of the dielectric tensor. The coefficients of the expansion are expressed as analytic functions of ω and θ. This allows to obtain approximated expressions of the wavevectors to any order of δ and to evaluate the truncation errors. Actual expressions of the determinant up to the 6th order of δ are explicitly given and the corresponding errors plotted. These results can be considered as an important generalization of the expressions obtained by a different technique in papers 4, 6. Actually in paper 6 a perturbative technique has been used which can be considered equivalent to an expansion of the determinant up to terms of δ.[2] In papers 4 the two-wave and the three-wave techniques have been employed, and thus the expressions of the wavevectors contain only terms in δ^2 and δ^4 respectively.

Furthermore, to obtain sufficiently simple results, in these papers other approximations have been made which limit their generality. In particular the results of paper 6 are valid only in the case of small incidence angles, while those of papers 4 require δ values of the order 0.01 or less. The expressions given in the present paper are analytically more involved but they are not bound by these limitations. Moreover, these expressions can be greatly simplified when one considers particular situations which allow further approximations.

An analysis of the Bloch wave solutions more detailed than the one done in paper 5 is also made. In particular a full discussion about the symmetry properties, polarization states and spectral composition of the waves is given.

2. BLOCH WAVES

The optical model is defined by the dielectric tensor

$$\epsilon = \begin{pmatrix} \epsilon_m(1 + \delta\cos 2qz) & \epsilon_m\delta\sin 2qz & 0 \\ \epsilon_m\delta\sin 2qz & \epsilon_m(1 - \delta\cos 2qz) & 0 \\ 0 & 0 & \epsilon_3 \end{pmatrix} \tag{1}$$

Symbols are listed below.

We consider a sample of cholesteric liquid crystal bounded by planes perpendicular to the helix axis, corresponding to a situation of most practical interest. When a plane wave incides on the sample, the wave inside the crystal can be represented as a sum of four elementary modes having the shape of a Bloch wave. If the incidence plane coincides with the (x, z) plane, each elementary mode can be represented as follows:

$$\begin{pmatrix} E_x \\ E_y \end{pmatrix} = \frac{1}{2}\exp i(\mathrm{K}_\perp x - \omega t) \sum_{n=-\infty}^{\infty} \begin{pmatrix} u_n + v_n \\ iu_n - iv_n \end{pmatrix} \exp[i(\mathrm{K}_\parallel + 2qn)z] \tag{2}$$

and

$$\begin{aligned} E_z &= -\frac{m}{\epsilon_3} H_y \\ H_z &= mE_y \\ H_y &= -i\frac{c}{\omega}\left(1 - \frac{m^2}{\epsilon_3}\right)^{-1} \frac{dE_x}{dz} \\ H_x &= i\frac{c}{\omega}\frac{dE_y}{dz} \end{aligned} \tag{3}$$

$\mathrm{K}_\parallel$ and $\mathrm{K}_\perp$ are the components of the wave vector **K** parallel and normal to the helix axis respectively. $\mathrm{K}_\perp$ coincides with the K_x component of the incident wave vector.

The quantity m appearing in eqs. (3) is given by the relation:

$$m = \frac{\mathrm{K}_\perp c}{\omega} = n_i \sin\theta_i \tag{4}$$

where θ_i is the incidence angle and n_i the external refractive index. The $\mathrm{K}_\parallel$ component is defined but for a quantity $2qn$, where $2qn$ is the modulus of a vector of the reciprocal lattice; i.e.

$$q = \frac{2\pi}{p}; \qquad p = \text{helix pitch} \tag{5}$$

The u_n and v_n coefficients define the amplitudes and the polarization states of the Fourier components of the mode, and satisfy the recurrent relations[5]

$$\begin{aligned} c_n v_{n-1} + a_n u_n + b_n v_n &= 0 \\ b_n u_n + a_n v_n + c_n u_{n+1} &= 0 \end{aligned} \tag{6}$$

where

$$a_n = a - a'(k+n)^2 \tag{7}$$

$$b_n = b - b'(k+n)^2 \tag{8}$$

$$c_n \equiv c = m'\delta\omega_n^2 \tag{9}$$

$$a = m'\left(1 - \frac{\overline{m}^2}{2}\right)\omega_n^2 \tag{10}$$

$$b = m'\frac{\overline{m}^2}{2}\omega_n^2 \tag{11}$$

$$a' = \frac{1}{2}\left(\frac{1}{m'} + m'\right) \tag{12}$$

$$b' = \frac{1}{2}\left(\frac{1}{m'} - m'\right) \tag{13}$$

$$m' = \left(1 - \frac{\overline{m}^2}{1-\delta'}\right)^{1/2}; \qquad \overline{m} = m\epsilon_m^{-1/2} \tag{14}$$

$$\delta = \frac{\epsilon_1 - \epsilon_2}{\epsilon_1 + \epsilon_2}; \qquad \delta' = \frac{\epsilon_m - \epsilon_3}{\epsilon_m}; \qquad \epsilon_m = \frac{\epsilon_1 + \epsilon_2}{2} \tag{15}$$

$$\omega_n = \frac{\omega}{2qc}\epsilon_m^{1/2} \tag{16}$$

$$k = \frac{K_{\parallel}}{2q} \tag{17}$$

As shown in ref. (5) the equations system (6) has non trivial solutions only if the component $K_{\parallel} = 2qk$ of the wave vector satisfies the following characteristic equation

$$\sin^4\pi k - 2U(\omega, \theta_i)\sin^2\pi k + V(\omega, \theta_i) = 0 \tag{18}$$

where[6]

$$\begin{aligned} 2U &= \sin^2(\pi k_\pi) + \sin^2(\pi k_\sigma) - \pi d_\pi \sin(2\pi k_\pi) - \pi d_\sigma \sin(2\pi k_\sigma) \\ V &= \sin^2(\pi k_\pi)\sin^2(\pi k_\sigma) - \pi d_\pi \sin(2\pi k_\pi)\sin^2(\pi k_\sigma) \\ &\quad - \pi d_\sigma \sin(2\pi k_\sigma)\sin^2(\pi \kappa_\pi) \end{aligned} \tag{19}$$

$$d_\pi = \lim_{k \to k_\pi} (k - k_\pi) D^*(k)$$

$$d_\sigma = \lim_{k \to k_\sigma} (k - k_\sigma) D^*(k) \tag{20}$$

$$D^*(k) = \det \begin{pmatrix} \cdot & \cdot & \cdot & \cdot & \cdot & \cdot & \cdot \\ 0 & \dfrac{c}{(k+n)^2 - k_\pi^2} & \dfrac{a - a'(k+n)^2}{(k+n)^2 - k_\pi^2} & \dfrac{b - b'(k+n)^2}{(k+n)^2 - k_\pi^2} & 0 & 0 & 0 \\ 0 & 0 & \dfrac{b - b'(k+n)^2}{(k+n)^2 - k_\sigma^2} & \dfrac{a - a'(k+n)^2}{(k+n)^2 - k_\sigma^2} & \dfrac{c}{(k+n)^2 - k_\sigma^2} & 0 & 0 \\ 0 & 0 & 0 & \dfrac{c}{(k+n+1)^2 - k_\pi^2} & \dfrac{a - a'(k+n+1)^2}{(k+n+1)^2 - k_\pi^2} & \dfrac{b - b'(k+n+1)^2}{(k+n+1)^2 - k_\pi^2} & 0 \\ \cdot & \cdot & \cdot & \cdot & \cdot & \cdot & \cdot \end{pmatrix} \tag{21}$$

and

$$k_\pi = m'\omega_n$$
$$k_\sigma = (1 - \bar{m}^2)^{1/2}\omega_n \tag{22}$$

3. EVALUATION OF k BY MEANS OF POWER SERIES EXPANSION

In ref. 5 the previously defined quantities d_π and d_σ have been evaluated by truncating the determinant D^*. However it is possible to show that D^* can be expanded to any order in a power series of the small parameter δ which represents the local dielectric anisotropy of the medium. An outline of the calculations is given in the Appendix. From the power series expansion the quantities d_π and d_σ are immediately obtained as:

$$d_\pi = A_\pi\delta^2 + B_\pi\delta^4 + \cdots \tag{23}$$

where

$$A_\pi = \frac{(m'\omega_n^2)^2}{2k_\pi(k_\pi^2 - k_\sigma^2)}\left(\frac{a_{-1}a_0}{Q_{-1}} + \frac{a_0a_1}{Q_1}\right)_{k=k_\pi} \tag{24}$$

$$B_\pi = \frac{(m'\omega_n^2)^4}{2k_\pi(k_\pi^2 - k_\sigma^2)}\left[\frac{a_{-2}a_0}{Q_{-2}Q_1} + \frac{a_{-1}a_1}{Q_{-1}Q_1} + \frac{a_0a_2}{Q_1Q_2} + \frac{a_{-1}a_0a_1}{Q_{-1}Q_1}\left(\frac{a_{-2}}{Q_{-2}} + \frac{a_2}{Q_2}\right)\right]_{k=k_\pi}$$
$$+ (m'\omega_n^2)^2 A_\pi \sum_{n=2}^{\infty}\left[\frac{a_{-n-1}}{Q_{-n-1}}\frac{a_{-n}}{Q_{-n}} + \frac{a_n}{Q_n}\frac{a_{n+1}}{Q_{n+1}}\right]_{k=k_\pi} \tag{25}$$

and

$$Q_n = Q_n(k) = \left[(k+n)^2 - k_\pi^2\right]\left[(k+n)^2 - k_\sigma^2\right] \tag{26}$$

Analogous expressions with k_σ instead of k_π are used for evaluating d_σ. The series in B_π can be rigorously evaluated by the method of residues; consequently the wave vector $\mathbf{k}$ can be evaluated by fully analytic, even if rather complicated, expressions.

A detailed analysis of the truncation errors with respect to k has been performed at various angles of incidence, with δ varying between 0 and 0.2 in the range of the low reflection bands. This analysis has

been performed up to the term containing δ.[8] Test values for k can be easily obtained through the numerical evaluation of the determinant D^*, owing to its very rapid convergence in the examined frequency range. For ω well below the onset of the first reflection band, the maximum truncation error is less than δ^n, where n is the first omitted term in the expansion (23). Between two contiguous reflection bands, the error is instead within the limits δ^n and δ^{n-2}, and is generally increasing with the order of the bands (see Figure 1). On the other hand the approximation becomes less accurate near and within any reflection bands. This case will be treated in Section 5.

Far from the reflection bands, and for all δ values corresponding to actual cholesteric liquid crystals, the expansion terms reported in eq. (23) are sufficient to derive very accurate k values. Finally, we notice that in this case both quantities d_π and d_σ are much smaller than unity. As a consequence, it can be shown that the characteristic equation can be approximated as follows

$$[\sin^2\pi k - \sin^2\pi(k_\pi - d_\pi)][\sin^2\pi k - \sin^2\pi(k_\sigma - d_\sigma)] \approx 0 \qquad (27)$$

which gives

$$k \approx \pm(k_\pi - d_\pi) + n; \qquad k \approx \pm(k_\sigma - d_\sigma) + n \qquad (28)$$

The errors affecting this approximation are plotted in Figure 2 versus ω at an intermediate incidence angle.

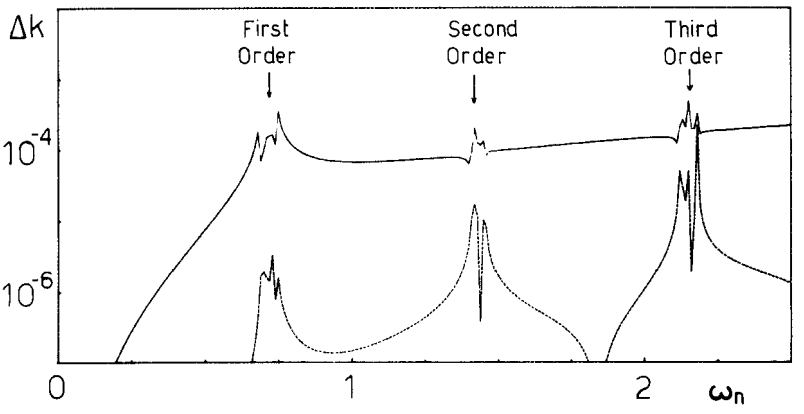

FIGURE 1 Truncation error Δk introduced in the evaluation of k by the δ^2 (full line) and δ^4 (dashed line) approximations. $\delta = \delta' = 0.05$, which correspond to $\epsilon_1 : \epsilon_2 : \epsilon_3 = 1.05 : .95 : .95$; $\bar{m} = \sqrt{2}/2$. Notice that the approximation is worse near to reflection bands.

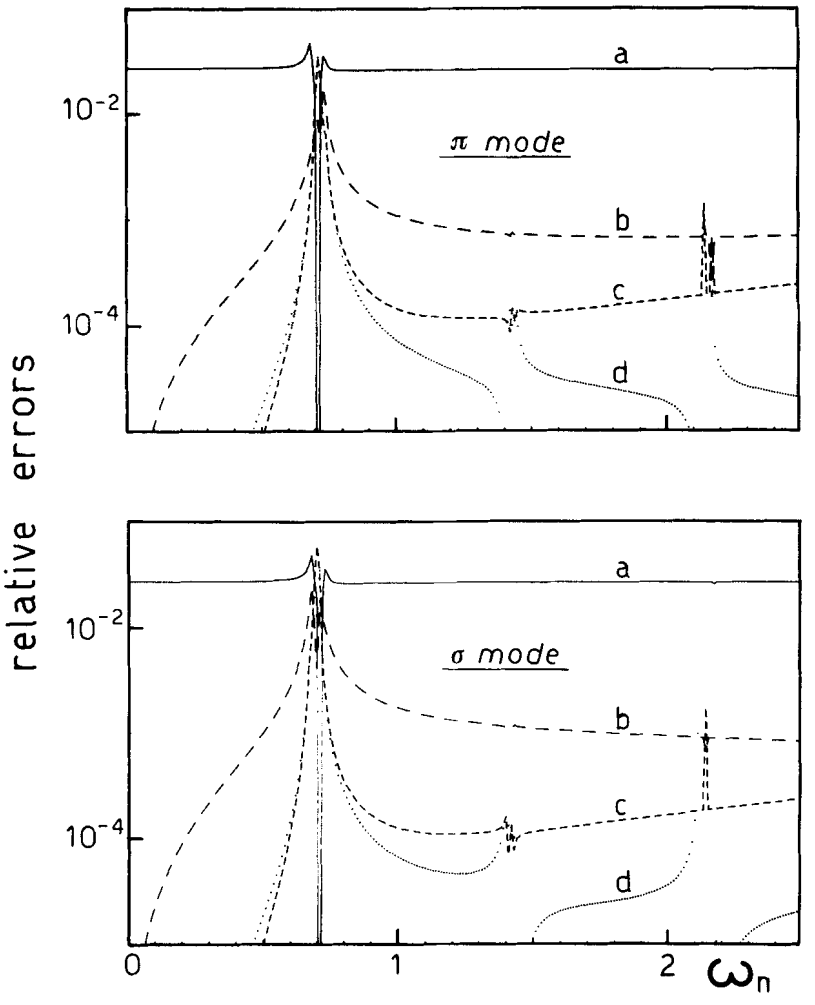

FIGURE 2 Relative errors introduced in the evaluation of k by eqs. (28) and (23) for the π and σ modes. The curves b, c, d refer to the zero, first and second order approximations respectively. The discontinuities correspond to reflection bands. In the instability regions the errors are at any approximation much less than the relative differences between the k values of π and σ modes plotted in a.

Notice that for $\delta \to 0$ the medium becomes homogeneous and anisotropic. In this case d_π and d_σ are zero and the possible values of $K_{\parallel}$ are $\pm 2qk_\pi$, and $\pm 2qk_\sigma$. The corresponding waves are π and σ polarized, i.e. with their electric field parallel and normal to the incidence plane respectively. We shall show that at large incidence angles the Bloch waves in a cholesteric l.c. are nearly of π or σ type, with the electric field nearly parallel or nearly normal to the incidence plane respectively. As shown by curves b) in Figure (2), the zero order approximation, which identifies the k values of the two modes with k_π and k_σ respectively, can be considered a good one. More generally we found that at medium and large incidence angles, and far from the reflection bands, the wavevectors can be evaluated with good approximation by the well known formulas of the anisotropic homogeneous media.

4. CLASSIFICATION OF THE SOLUTION OF THE CHARACTERISTIC EQUATION

As observed in ref. 5, an interesting classification of the Bloch waves can be obtained by a simple analysis of the characteristic equation. Such an analysis is here reformulated in a new way which is both simpler and of more general validity of the previous one, which made an unnecessary distinction between the two cases of real and imaginary coefficients of the characteristic equation.

Actually, if the components of the dielectric tensor are real (i.e. the energy dissipation is neglected), such coefficients are always real even in the case where all the matrix elements of D^* are complex. The proof is based on the following facts:

a) all the quantities appearing in the matrix elements of D^* are real, except those containing m' and k_σ, which, according to eqs. (14) and (22) become pure imaginary for sufficiently large incidence angles;

b) only even powers of m' appear in the expansion terms of D^*;

c) the values of the coefficients U and V of the characteristic equation do not actually depend on k_σ, whose choice is a pure matter of convenience, as discussed in ref. (5).

The characteristic equation (18) can be written in the equivalent form

$$\cos^2(2\pi k) - 2U'(\omega, \theta_i)\cos(2\pi k) + V'(\omega, \theta_i) = 0 \qquad (29)$$

where

$$U' = 1 - 2U; \qquad V' = 1 - 4U + 4V \tag{30}$$

The equation (29) gives two roots for $\cos(2\pi k)$ and thus four sets of characteristic values for k

$$\begin{aligned} k_1^+ &= \{k_1 + n\}; & k_2^+ &= \{k_2 + n\} \\ k_1^- &= \{-k_1 + n\}; & k_2^- &= \{-k_2 + n\} \end{aligned} \tag{31}$$

For each set, eqs. (6) have a unique independent solution, the characteristic exponent $K_{\parallel} = 2qk$ being defined but for an integer multiple of $2q$, according to eq. (2). Furthermore we observe that the two solutions corresponding to k_i^+ and k_i^- are simply related one to the other. For each value of the coefficients U' and V', i.e. for each point of the (ω, θ_i) plane, only two really independent solutions exist, as expected on the basis of the polarization properties of the electromagnetic waves. For U' and V' real the following cases may occur:

A) $\cos(2\pi k)$ is real and its modulus less than 1. The k exponent is real. The corresponding solution is stable and represents waves which propagate without attenuation.

B) $\cos(2\pi k)$ is real and its modulus larger than 1. The k exponent is complex, i.e. $k = k' + ik''$. The corresponding solution is unstable and represents a damping wave along the z axis, the amplitude attenuation constant being $2qk''$ and the attenuation length

$$\zeta = (2qk'')^{-1}$$

The real part of k is integer or semi-integer; thus

$$K'_{\parallel} = nq \tag{32}$$

Noting that the reciprocal lattice of the helicoidal structure is represented by points on the z axis at distance $2q$, we conclude that equation (32) is the condition to have the Bragg reflection.

When both solutions are of type B, a sample whose thickness is much larger than ζ gives total reflection irrespective of its polarization. If one solution is of type B and the other of type A the sample gives selective reflection.

C) The discriminant $U'^2 - V'$ of the characteristic equations is negative. The two roots are conjugate, and the four sets of characteris-

tic values are

$$k_1^+ = \{k' + ik'' + n\}; \qquad k_2^+ = \{-k' + ik'' + n\}$$
$$k_1^- = \{-k' - ik'' + n\}; \qquad k_2^- = \{+k' - ik'' + n\}$$

The solutions are unstable. A sample having a thickness large with respect to ζ gives always total reflection. The solutions k_i^+ give waves with attenuation along positive direction of the z axis, while for the others the attenuation is in the opposite direction. We can also observe that the real part of $K_{\parallel}$ does not satisfy the Bragg condition. However the difference between a vector of the k_1^+ set and a vector of the k_2^- set is a vector of the reciprocal lattice (Figure 3b).

D) At the boundaries between zones of different type the characteristic equation gives degenerated roots for k. In this case a basic set of Bloch solutions for the Maxwell equations no longer exists. The different cases which can occur are represented in Figure 4. At the boundary between (A + A) and (A + B) type regions only three of the four sets of solutions are independent. At the boundary of the C type region only two are independent. Where two boundary lines met, i.e. in the $(-1, +1)$, $(+1, +1)$ and $(0, -1)$ points, only one Bloch solution exists.

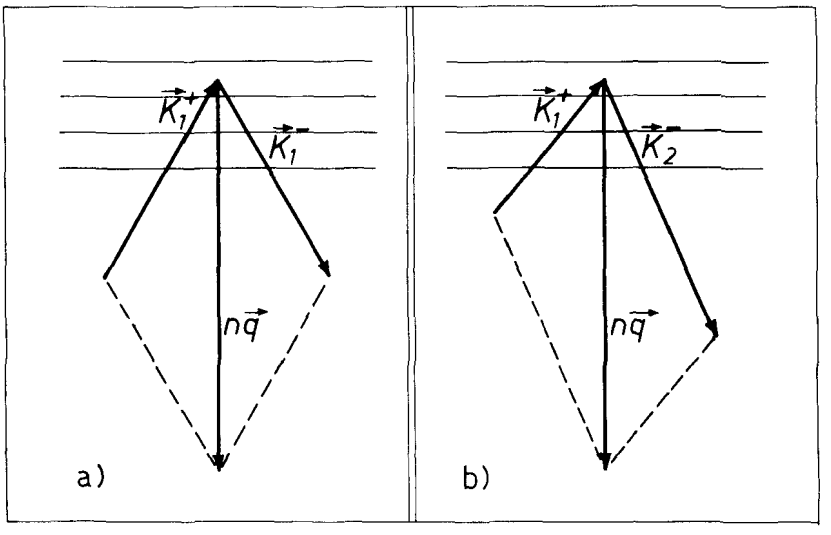

FIGURE 3 Wave vectors corresponding to refraction from B type (a) and C type (b) instabilities respectively. $n\mathbf{q}$ is a vector of the reciprocal lattice.

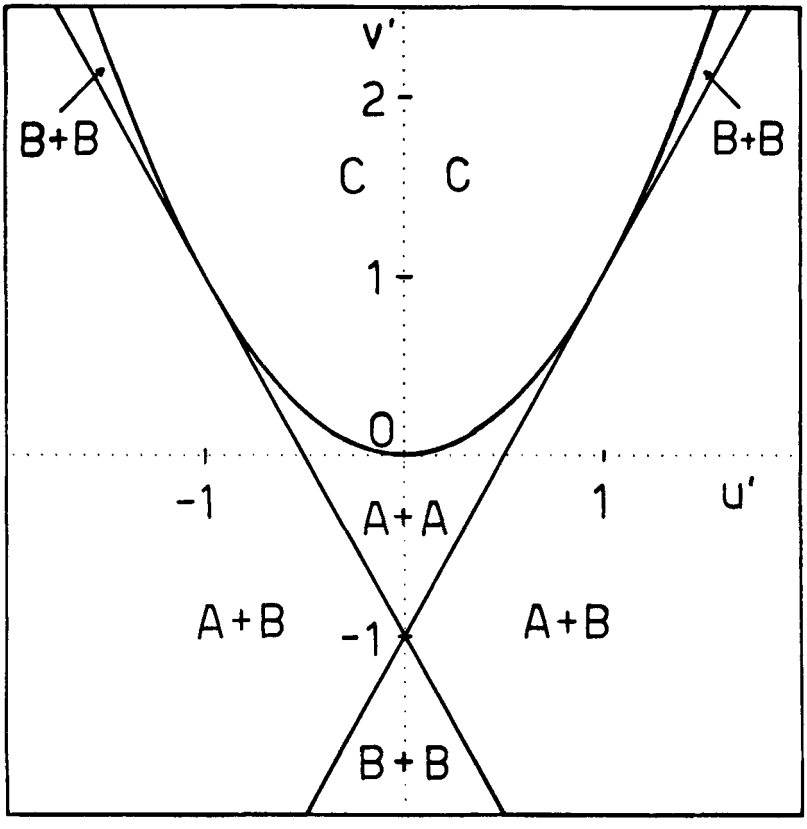

FIGURE 4 Stability and instability of the two modes in the (U', V') plane. The boundary of the C type instability region satisfies the equation $V' = U'^2$, the straight lines have eqs. $V' = -1 \pm 2U'$ and are the loci of points where one of the modes goes from a stable solution to an unstable one of type B.

5. ANALYSIS OF THE FIRST REFLECTION BANDS

The fact that the characteristic equation has degenerated roots within the instability regions explains why the perturbation expansion gives the worst results near the reflection bands. Figures 5 and 6 show both the exact values of k and the approximated ones for different incidence angles and $\delta = 0.1$. The approximation is to the order of δ^2 for the first band, and to the order of δ^4 for the higher order bands, where the δ^2 approximation cannot be used.[4] Such approximations give a rather good qualitative description but they are not suitable for calculating the reflection properties of the bands, which are related to the imaginary part of k. The expansions to δ^4 or to δ^6, instead, give

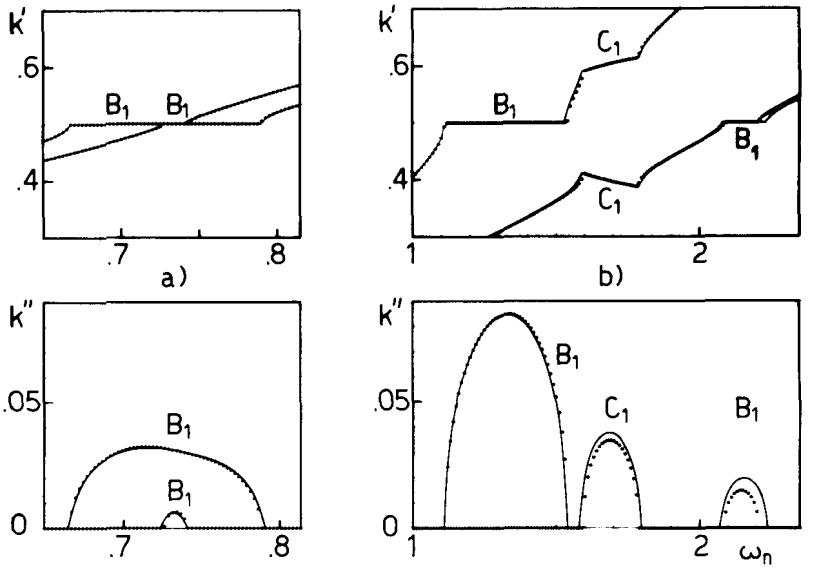

FIGURE 5 Plots of the real and imaginary part, k' and k'', of the characteristic vector near the first order reflection band, for $\delta = \delta' = 0.1$. In (a), where $\overline{m} = \sqrt{2}/2$, corresponding to intermediate incidence angles, an interval appears where both modes have a B type instability. In (b), where $m = \sqrt{0.85}$, corresponding to very high incidence angles, the first order band splits in a triplet. The lateral peaks correspond to B type instabilities, while the central peak, which is common to both modes, is of C type. Full lines are the exact k values while dotted lines are the values given by the δ^2 approximation.

values practically indistinguishable from the exact ones. However the errors grow rapidly when δ becomes larger than 0.1. Actually, already for $\delta = 0.2$ the second reflection band is well described only by an expansion to the δ^8 order: when $\delta > 0.1$ the study of the reflection bands of order > 1 requires very complicated analytic expressions.

A short description of the structure and polarization properties of the reflection bands follows.

The bands of order $n > 1$ are triplets, the lateral peaks being related to Bragg instabilities and the central one to a C type instability. For a given θ_i value the three instability zones of the same band have comparable width and comparable attenuation coefficients, as shown in Figure 6. Therefore for unpolarized incident light the reflection band contains three peaks whose strengths are of the same order of magnitude. For polarized light, instead, the strength may be greatly different because the lateral peaks give selective reflection, while the central one gives reflection of light irrespective of its polarization. Figure 6 shows also that the peak strength increases rapidly with the

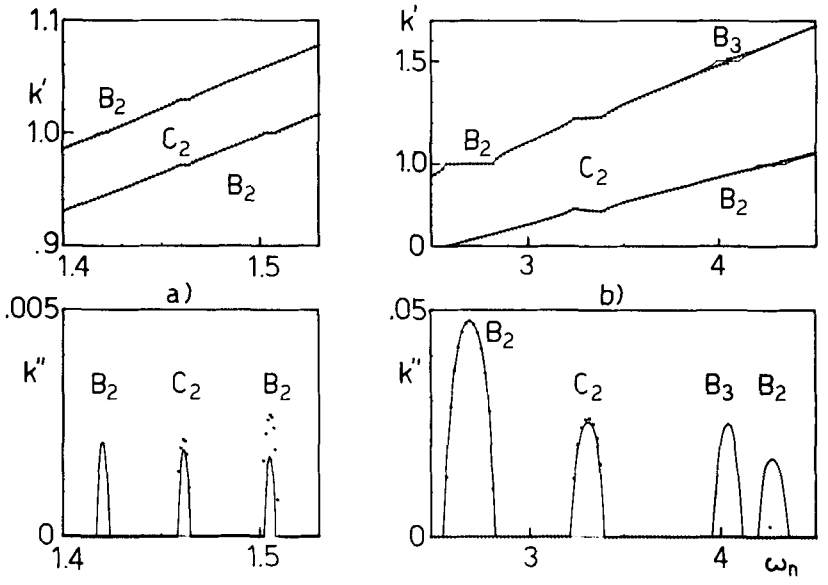

FIGURE 6 Same as for Figure 5, but referred to the second order reflection band. Here dotted lines are the k values given by the δ^4 approximation. Notice that at small incidence angles (Figure 6a), the attenuation constant k'' becomes very small (and vanishes at normal incidence).

incidence angle, and that at very large incidence angles, peaks of different order overlap.

The first order peak has a more complex structure. At low and medium incidence angles a frequency range where both modes have an instability of B type exists (Figure 5a), while at large incidence angles the band has the same behaviour of the reflection bands of higher order, with three well separated peaks, the central one being of C type (Figure 5b).

6. POLARIZATION PROPERTIES AND SPECTRAL COMPOSITION OF BLOCH WAVES

In the following we stress the most important differences between the well known case of normal incidence[8] and that of oblique incidence. The stability regions and the instability ones are separately treated. In a stable region and for normal incidence the light is locally elliptically polarized, the ellipse having always the same shape and rotating along z in such a way that its axes coincide everywhere with the local axes of the dielectric tensor.

For oblique incidence it is convenient to consider the ellipse described locally by the x and y components of the electric field. The shape of this ellipse is a periodic function of z with the same periodicity of the cholesteric structure; its axes coincide with the local axes of the dielectric tensor only on those planes where the dielectric tensor has axes parallel and normal to the incidence plane. With previously used symbols such planes have equation $z = Lp/4$ where L is any integer. Such a property allows to select the polarization state of the incident light in order to excite only one of the internal modes. We notice that such a property does not depend on the symmetries of the propagation equations, but is a consequence of the fact that for real k all u_n, v_n coefficients in Eq. (2) are real. The ellipse shape is in fact given by

$$\begin{pmatrix} X(z) \\ Y(z) \end{pmatrix} = \sum_n \begin{pmatrix} x_n \\ -iy_n \end{pmatrix} \exp(2iqnz) = \frac{1}{2} \sum_n \begin{pmatrix} u_n + v_n \\ iu_n - iv_n \end{pmatrix} \exp(2iqnz) \tag{33}$$

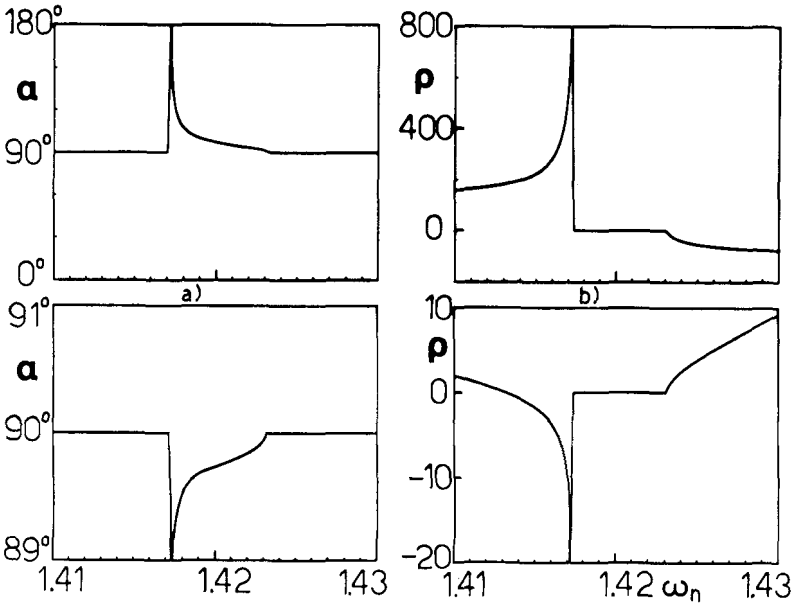

FIGURE 7 The curves define the polarization states of the light in the $z = 0$ (upper curves) and in the $z = p/4$ (lower curves) planes, around the second order Bragg instability for the σ type mode. α is the angle between the major axis of the ellipse and the incidence plane, ρ the axis ratio. In the instability region $\rho = 0$, i.e. linear polarization occurs, and the azimuth rotates from the direction of one of the principal axes of the dielectric tensor to the other one. In the stability regions $\alpha = 90$ deg: the axes of the ellipse coincide with the principal axes of the dielectric tensor. $\epsilon_1 : \epsilon_2 : \epsilon_3 = 1.1 : 0.9 : 0.9$.

because the factor $\exp i(K_\perp x + K_\parallel z - \omega t)$ gives the same phase change to both X and Y components. It is easily understood that for u_n, v_n reals and $z = Lp/4 = (L/4)(2\pi/q)$, the phase difference between the X and Y component is $\pm\pi/2$.

It is well known that for normal incidence the minor axis of the ellipse reduces to zero at the boundaries of the instability band. Within this band the local polarization is linear, with the azimuth rotating from the direction of one of the principal axes of the dielectric tensor to the direction of the other one, as ω increases going through the whole band. At oblique incidence analogous properties are met through an instability region of B type, only in the $z = Lp/4$ planes. At the boundaries of the zone the electric field is parallel or normal to the incidence plane. To demonstrate this property we note that Eqs. (6) do not vary by changing k in $-k$, n in $-n$ and by interchanging u and v. If a solution $S^+ = (k; a_n, b_n)$ exists, where a_n and b_n are the values of u_n and v_n respectively, also the solution $S^- = (-k; b_{-n}, a_{-n})$ does exist. At the boundaries of a B type instability the two solutions coincide. For the instability zones of even order the characteristic value k is an integer, which can be chosen as zero. The coincidence of

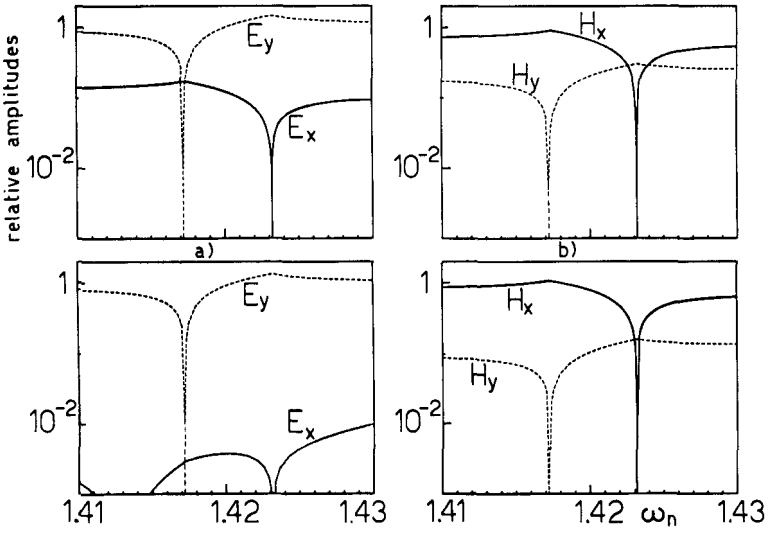

FIGURE 8 Amplitudes of the electric and magnetic fields components evaluated in the $x = 0$ plane (upper figures) and in the $z = p/4$ plane (lower figures), in the same conditions of Figure 7. The boundaries of the instability region are where one of the components is zero. Notice that a nodal (ventral) plane for the E_x component is a ventral (nodal) plane of the H_y component, which means standing waves (analogously for the E_y and H_x components), and that the E_y component is nearly everywhere dominant.

the solutions S^+ and S^- implies

$$(a_n, b_n) = \pm(b_{-n}, a_{-n})$$

and

$$\begin{pmatrix} x_n \\ y_n \end{pmatrix} = \pm \begin{pmatrix} x_{-n} \\ -y_{-n} \end{pmatrix}$$

Depending on the sign, the $z = Lp/4$ planes are nodal planes for the X or for the Y component. For instance by choosing the sign $+$, the Eq. (33) gives

$$\begin{pmatrix} X(z) \\ Y(z) \end{pmatrix} = \begin{pmatrix} x_0 \\ 0 \end{pmatrix} + \sum_{n=1}^{\infty} \begin{pmatrix} 2x_n \cos 2qnz \\ 2y_n \sin 2qnz \end{pmatrix} \tag{34}$$

In the $z = Lp/4$ planes, the Y component is therefore zero and the electric field is in the incidence plane.

For the bands of odd order, where k is semi-integer, the demonstration is analogous.

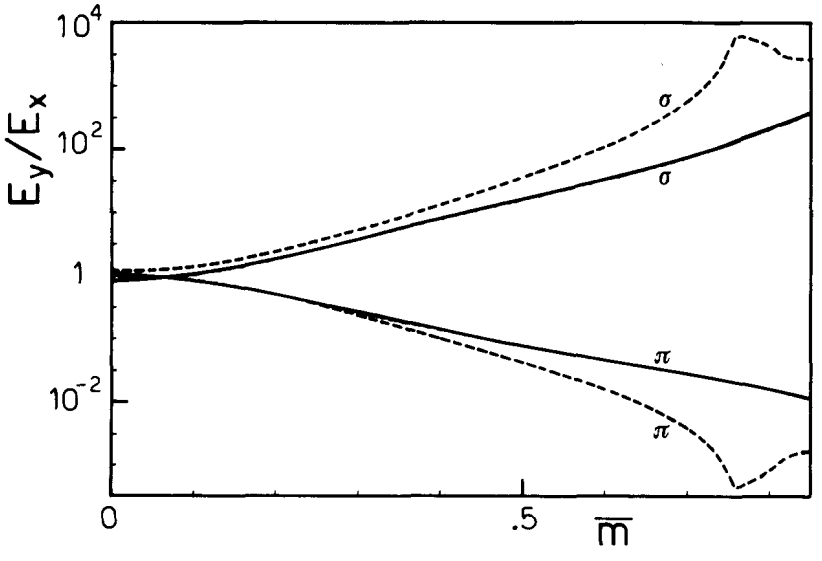

FIGURE 9 Ratios between the y and x components of the electric field for the two modes evaluated in the $z = 0$ (full lines) and in the $z = p/4$ (dashed lines) planes and for $\omega_n = 0.9$. The abscissa coincides with $\sin\theta_i$ if the external medium has a refractive index $n_i = ((\epsilon_1 + \epsilon_2)/2)^{1/2}$. Notice that for $\theta_i < 0.1$ rad the modes have nearly the same characteristic of the normal incidence, while for larger angles they rapidly separate and their polarization become of π and σ type respectively.

In order to understand the Bragg reflection properties as a function of the polarization state of the incident wave, we must note that the local linear polarization is due to the superposition of Fourier components having the same amplitude and wave vectors of opposite z-components. Therefore the phase relation between **E** and **H** are those characterizing a standing wave.

Outside of the planes $z = Lp/4$ the behaviour of the X and Y components is more complex. However we observe that at large incidence angles the electric fields of the two modes have a very weak and a very strong y component respectively; i.e. they are predominantly π and σ polarized (Figure 9).

For what concerns the spectral composition of the modes, we observe that at normal incidence all the Fourier components are zero, except two of them; at oblique incidence also the other Fourier component are present. However, far from the instability regions one of the Fourier components is predominant. Near or inside the instability regions there are at least two components of comparable amplitude (Figure 10).

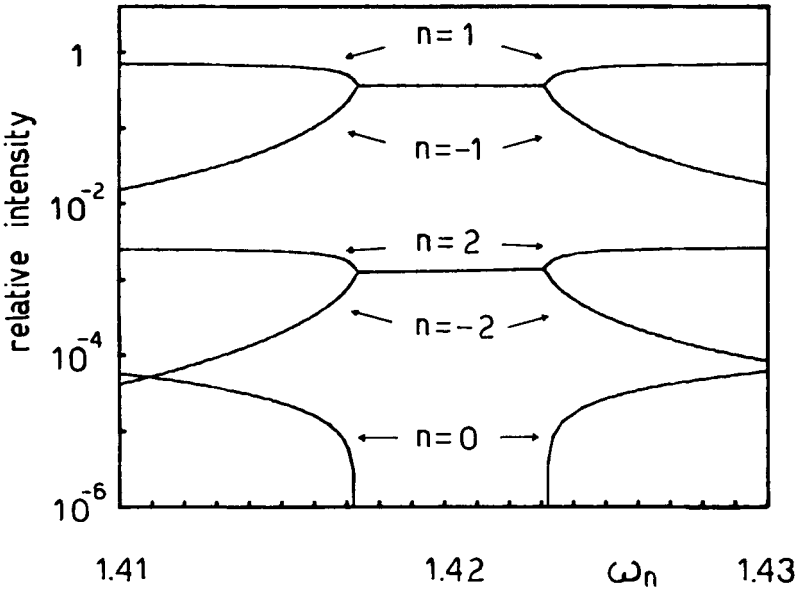

FIGURE 10 Relative intensity of the Fourier components of σ mode evaluated in the same conditions of Figure 7. The curves represent the z component absolute values of the Poynting vector. In the instability region, the components with opposite indices have the same modulus but opposite sign. In the stability regions they rapidly separate and one of the components becomes dominant.

7. CONCLUSIONS

As a conclusion, we stress the following points:

a) The polarization state of Bloch waves at large incidence angles is substantially different from the one at small angles. For large incidence angles, a light beam gives rise to two waves, whose polarization states are predominantly of type π and σ, respectively. By lowering the incidence angle, both waves gradually assume the nearly circular polarization state characterizing the normal incidence.

The expansion of k in a series of powers of the small parameter δ^2, given in the present work, is a very general algorithm which is particularly suitable to describe the case of large incidence angles, since the zero order approximation corresponds to the case of π and σ type polarizations. In fact, in the limit $\delta \to 0$, the two Bloch waves reduce respectively to the extraordinary and ordinary beams of homogeneous anisotropic media.

b) Within the instability regions, each Bloch wave contains Fourier components occurring in pairs whose Poynting vectors have the same modulus and z-components of opposite sign.

When δ is lower than 0.2, only one of these pairs dominates on all other pairs. According to this result, it is conceivable that in this case the optical properties of the cholesteric l.c. can be studied with a good approximation within the framework of a dynamical theory. In the immediate neighborhood of any instability region, one component of the dominant pair becomes rapidly negligible with respect to the other one, as clearly shown in Figure 10. The dominant component is elliptically polarized. At large incidence angles, the elliptical polarization tends to collapse into a rectilinear one. In this condition and far enough from the instability regions, the Bloch waves can be roughly approximated as plane waves rectilinearly polarized in π and σ planes, whose wave vectors can be evaluated with a good approximation by the well known formulas of the anisotropic homogeneous media.

It is important to notice that in any case only few components of the Bloch waves have not negligible amplitude. Owing to this fact, the evaluation of the amplitude of the Fourier components becomes easier, because, with good approximation, only few of the Eqs. (6) are to be retained. In addition, once k is determined through the characteristic equation, the system (5) simply reduces to a linear system of equations with constant coefficients. For this reason, most of this work and of the preceding one is devoted to the resolution of the characteristic equation.

APPENDIX

The series expansion of $D^*(k)$ in terms of powers of δ^2 is made possible, and relatively easy, by the following properties:

a) The matrix elements which contain the quantity c are proportional to δ;

b) all the other elements satisfy the following relation:

$$\det\begin{pmatrix} \dfrac{a - a'(k+n)^2}{(k+n)^2 - k_\pi^2} & \dfrac{b - b'(k+n)^2}{(k+n)^2 - k_\pi^2} \\ \dfrac{b - b'(k+n)^2}{(k+n)^2 - k_\sigma^2} & \dfrac{a - a'(k+n)^2}{(k+n)^2 - k_\sigma^2} \end{pmatrix} = 1 \tag{A1}$$

c) if a term of the expansion of $D^*(k)$ contains the element $c[(k+n)^2 - k_\sigma^2]^{-1}$ it also contains the element $c[(k+n+1)^2 - k_\pi^2]^{-1}$ and thus only even powers of δ are present.

One can thus write

$$D^*(k) = 1 - D_2\delta^2 + D_4\delta^4 - D_6\delta^6 + \cdots \tag{A2}$$

where

$$D_2 = (m'\omega_n^2)^2 \sum_{n=-\infty}^{\infty} \frac{a_n}{Q_n}\frac{a_{n+1}}{Q_{n+1}} \tag{A3}$$

$$D_4 = (m'\omega_n^2)^4 \left[\sum_{n=-\infty}^{\infty} \frac{a_{n-1}}{Q_{n-1}}\frac{1}{Q_n}\frac{a_n}{Q_{n+1}} + \sum_{n=-\infty}^{\infty}\sum_{m=n+2}^{\infty} \frac{a_n}{Q_n}\frac{a_{n+1}}{Q_{n+1}}\frac{a_m}{Q_m}\frac{a_{m+1}}{Q_{m+1}} \right] \tag{A4}$$

$$D_6 = (m'\omega_n^2)^6 \left[\sum_{n=-\infty}^{\infty} \frac{a_n}{Q_n}\frac{1}{Q_{n+1}}\frac{1}{Q_{n+2}}\frac{a_{n+3}}{Q_{n+3}} + \sum_{n=-\infty}^{\infty}\sum_{m=n+2}^{\infty} \frac{a_{n-1}}{Q_{n-1}}\frac{1}{Q_n}\frac{a_{n+1}}{Q_{n+1}}\left(\frac{a_m}{Q_m}\frac{a_{m+1}}{Q_{m+1}} + \frac{a_{-m}}{Q_{-m}}\frac{a_{-m-1}}{Q_{-m-1}}\right) + \sum_{n=-\infty}^{\infty}\sum_{m=n+2}^{\infty}\sum_{l=n+m+2}^{\infty} \frac{a_n}{Q_n}\frac{a_{n+1}}{Q_{n+1}}\frac{a_m}{Q_m}\frac{a_{m+1}}{Q_{m+1}}\frac{a_l}{Q_l}\frac{a_{l+1}}{Q_{l+1}} \right] \tag{A5}$$

and

$$Q_n \equiv Q_n(k) = \left[(k+n)^2 - k_\pi^2\right]\left[(k+n)^2 - k_\sigma^2\right] \qquad \text{(A6)}$$

The term $D_2\delta^2$ in Eq. A2 is a sum, over n, of products of the type

$$\frac{a - a'(k+n)^2}{(k+n)^2 - k_\pi^2} \quad \frac{c}{(k+n)^2 - k_\sigma^2}$$

$$\frac{c}{(k+n+1)^2 - k_\pi^2} \quad \frac{a - a'}{(k+n+1)^2 - k_\sigma^2}$$

This gives immediately the expression of D_2 given in Eq. A3. For the calculation of D_4 one must take into account terms containing products of the type

$$\frac{c}{(k+n)^2 - k_\sigma^2} \quad \frac{c}{(k+n)^2 - k_\pi^2}$$

$$\frac{c}{(k+n+m)^2 - k_\sigma^2} \quad \frac{c}{(k+n+m)^2 - k_\pi^2}$$

where m ranges from 1 to ∞.

In Eq. A4 the first sum appearing within square brackets comes from the contribution of the terms containing products where $m = 1$, while the double sum is relative to all the other terms.

The coefficient D_6 and the subsequent ones are obtained in a similar way. From these results it becomes easy to obtain the quantities

$$d_\pi = \lim_{k \to k_\pi} (k - k_\pi) D^*(k); \qquad d_\sigma = \lim_{k \to k_\sigma} (k - k_\sigma) D^*(k)$$

appearing in the text.

It can be noticed that all the series appearing in the coefficients $D_2, D_4 \ldots$, can be summed up by the residue method. For instance

$$\sum_{n=-\infty}^{\infty} \frac{a_n}{Q_n} \frac{a_{n+1}}{Q_{n+1}}$$

$$= \pi \frac{a - a'k_\pi^2}{2k_\pi\left(k_\pi^2 - k_\sigma^2\right)} \left(\frac{a_{-1}}{Q_{-1}} + \frac{a_1}{Q_1} \right)_{k=k_\pi} \frac{\sin 2\pi k_\pi}{\sin \pi(k_\pi - k) \sin \pi(k_\pi + k)}$$

$$+ \pi \frac{a - a'k_\sigma^2}{2k_\sigma\left(k_\sigma^2 - k_\pi^2\right)} \left(\frac{a_{-1}}{Q_{-1}} + \frac{a_1}{Q_1} \right)_{k=k_\sigma} \frac{\sin 2\pi k_\sigma}{\sin \pi(k_\sigma - k) \sin \pi(k_\sigma + k)} \qquad \text{(A7)}$$

For the other series we must rewrite the terms in such a way to obtain sums varying from ∞ to $-\infty$.

Finally we can observe that the two-wave and three-wave approximations used in papers (4) correspond to a truncation of the determinant $D^*(k)$, and thus to a truncation of the series A2, to terms in δ^2 and δ^4 respectively. Furthermore all the series appearing in the expressions of the coefficients D_2 and D_4 are also truncated.

References

1. D. W. Berreman, *J. Opt. Soc. Am.*, **62**, 502 (1972).
2. D. Taupin, *J. Phys. (France)*, **30**, C4-32 (1969).
3. R. Dreher and G. Meier, *Phys. Rev. A*, **8**, 1616 (1973).
4. V. A. Belyakov and V. D. Dmitrienko, *Sov. Phys.—Solid State*, **15**, 1811 (1974); V. E. Dmitrienko and V. A. Belyakov, *Sov. Phys.—Solid State*, **15**, 2365 (1974).
5. C. Oldano, E. Miraldi, P. T. Valabrega, *Phys. Rev. A*, **27**, 3291 (1983).
6. T. H. Sterling and C. F. Hayes, *Mol. Cryst. Liq.*, **43**, 279 (1977).
7. In ref. (5) indices a and b instead of π and σ, and a normalized frequency $\omega_n = ((\epsilon_1 + \epsilon_2)/2)^{+1/2}\omega_r$ instead of ω_r, are used. The new formalism evidences the polarization states of the modes, and greatly simplifies the expressions of the other quantities.
8. For a detailed bibliography on optical properties of cholesteric l.c. see: Handbook of Liquid Crystals, H. Kelker and R. Hatz, Verlag Cehemie, Weinheim, 1980.